Chapter 14

Special ℓ_1-graphs

14.1 Equicut ℓ_1-graphs

In the first half of this chapter we follow [DePa01], where proofs of results below can be found.

A graph G is an *equicut graph* if it admit an l_1-embedding, such that the equality holds in the left-hand side of the inequality (1.2) of chapter 1, concerning the size $s(d_G)$ of this embedding. Below $s(d_G)$ means the size of such equicut embedding. This means that, for such a graph, every S in the equality (1.1) of chapter 1 corresponds to an *equicut* $\delta(S)$, i.e. satisfy $a_S \neq 0$ if and only if S partitions V into parts of size $\lceil \frac{n}{2} \rceil$ and $\lfloor \frac{n}{2} \rfloor$, where $n = |V|$.

Remind that a connected graph is called *2-connected* (or *2-vertex-connected*) if it remains connected after deletion of any vertex.

Lemma 14.1

An equicut graph with at least four vertices is 2-connected.

This lemma implies the following

Corollary 14.1

For any equicut graph G with $n \geq 4$ vertices, we have

$$2 - \frac{1}{\lceil \frac{n}{2} \rceil} \leq s(d_G) \leq \frac{n}{2}$$

with equality on the left-hand side if and only if $G = K_n$, and on the right-hand side if and only if $G = C_n$.

The condition $n \geq 4$ is necessary in the statements above. Indeed, $s(d_{P_3}) = 2 > s(d_{C_3}) = \frac{3}{2}$. Note, that P_2 and P_3 are the only equicut trees. Also, $W(C_5) = 15 < W(P_{\{123452\}})$ and $s(d_{C_5}) = \frac{5}{2} < s(d_{P_{\{123452\}}})$, where

$P_{\{123452\}}$ denotes the circuit on 2,3,4,5 with an extra edge attached to the vertex 2.

Remark 14.1 G is an equicut graph if there is a realization with the binary matrix F with the column sums $\lceil \frac{n}{2} \rceil$ or $\lfloor \frac{n}{2} \rfloor$. If, instead of this condition, we asked that any *row* of F has exactly k 1's, then we obtain other special ℓ_1-graph. Namely, one which is embedded isometrically, up to scale λ, into the Johnson graph $J(m,k)$. It was observed by Shpectorov, that such graphs can be recognized in polynomial time using the algorithm in [DeSh96], but we are not aware of any similar characterization of the equicut graphs. It is easy to see, that any graph G, which is embedded isometrically, up to scale λ, into hypercube H_m, is embedded also isometrically, up to scale λ, into Johnson graph $J(2m,m)$. In fact, let any vertex v of G be addressed by corresponding subset A_v of a given m-set; then one can address v by the union of A_v and the image of its complement in a bijection of the given m-set on some m-set, which is disjoint with given one. The columns "$J(m,k)$?" of Tables 4.1, 4.2 give all embeddings of Q into $J(m,k)$, where Q is anyone amongst Platonic polyhedra, semi-regular polyhedra or their duals.

Call an equicut ℓ_1-graph an *antipodal doubling* if its realization in H_m (i.e. the above (0,1)-matrix F) has the form $F = \begin{pmatrix} A & O \\ J-A & J' \end{pmatrix}$, where A is $\frac{n}{2} \times m'$ (0,1)-matrix, J, J' are matrices consisting of 1's only and O is $\frac{n}{2} \times (m-m')$ matrix consisting of 0's.

If, moreover, the matrix A is a realization, with the same scale λ, of a graph G', then it is straightforward to check, that J' has $\lambda(d(G')+1)-n$ columns, where $d(G)$ is diameter of G. Note that Double Odd graph DO_{2s+1} (see, for example, DO_5 on Figure 14.1) with $s \geq 3$ is an example of antipodal doubling with the matrix A not corresponding to the realization of a graph G', for any decomposition of F into the above form.

Remark 14.2 An antipodal doubling is exactly an ℓ_1-graph, that admits an antipodal isomorphism, i.e. it has a central symmetry (for any vertex, there is exactly one other on the distance equal to the diameter) and the mapping of all vertices into their antipodes is an isomorphism. Antipodal extensions of arbitrary ℓ_1-metrics was considered in [DeLa97], chapter 7.2.

In order to investigate, when one can construct an ℓ_1-graph from an ℓ_1-graph via the antipodal doubling (see Theorem 14.1 below), let us introduce the following definition. For a graph $G=(V,E)$, define its *diametral*

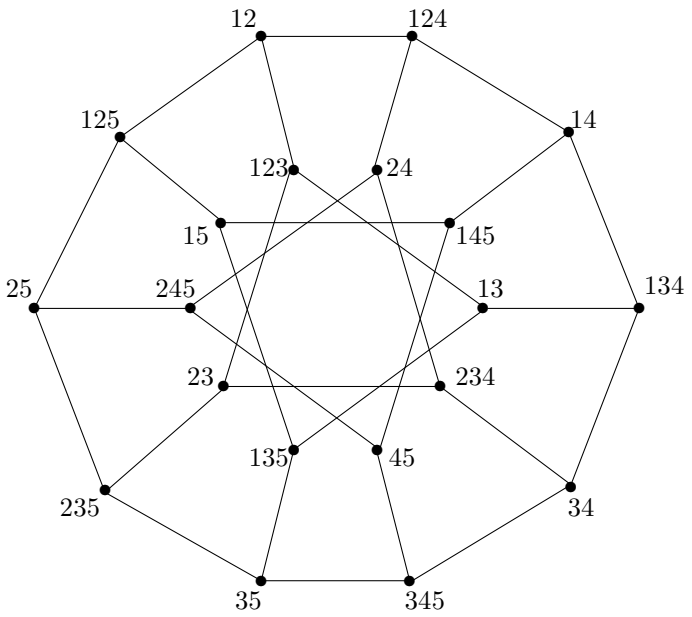

Fig. 14.1 **Double Odd graph DO_{2s+1} with $s = 2$**

doubling as the graph $\Box G$ with the vertex-set $V^+ \cup V^-$ (where V^+ and V^- are two copies of V) and the adjacency is as follows: u^a is adjacent to v^b if $a = b$ and $(u, v) \in E$, or if $a \neq b$ and $d_G(u, v) = d(G)$, where $a, b \in \{+, -\}$.

Lemma 14.2 *The subgraphs of $\Box G$, induced on V^+ and V^-, are isometric to G if and only if*

$$d_G(u, v) \leq 2 + d_G(w_1, w_2) \quad \text{for any } u, v, w_1, w_2 \in V, \text{ satisfying } d_G(u, w_1) = d_G(v, w_2) = d(G). \tag{14.1}$$

Lemma 14.3 *Let G satisfy the condition of above lemma. Then*

$$d_{\Box G}(u^+, v^-) = d(G) + 1 - d_G(u, v) \tag{14.2}$$

if and only if any geodesic in G lies on a geodesic of length $d(G)$.

Certain properties of G are inherited by $\Box G$.

Lemma 14.4 *Let G be a graph satisfying equations (14.1) and (14.2). Then $\Box G$ satisfies $d(\Box G) = d(G) + 1$, equations (14.1) and (14.2).*

If $d(G) = 2$, then G satisfies (14.1). Moreover, $G \neq K_n$ satisfies (14.2), unless it has an edge (u, v) with $G_u = G_v$, where G_u is the subgraph of G induced by the neighborhood of the vertex u. In particular, the strongly regular graphs, considered below, satisfy (14.1) and (14.2); note, that ℓ_1-graphs form a rather small sub-family of strongly regular graphs.

Not always the graph $\square G$ defines uniquely the graph G, from which it was constructed. It can be that $\square G' = \square G$ for $G \neq G'$. See below for many examples of this situation. But the graphs G and G' are related by the following graph operation. The *diametral switching* of a graph G with respect to $S \subset V$ is a graph G' that is obtained from G by retaining the edges that lie within $(S \times S) \cup ((V - S) \times (V - S))$ and replacing the set of edges from $S \times (V - S)$ with the set $\{(u, v) \in S \times (V - S) : d_G(u, v) = d(G)\}$.

Note that *Seidel switching* is an operation, that coincides with the diametral switching for graphs of diameter two.

Theorem 14.1 *Let G be an ℓ_1-graph. Then $\square G$ is an ℓ_1-graph if G satisfies (14.1), (14.2) and*

$$s(d_G) \leq d(G) + 1. \tag{14.3}$$

Moreover, if $\square G$ is an ℓ_1-graph, then it holds:

(i) $d(\square G) = d(G) + 1$, $\square G$ satisfies equations (14.1), (14.2) and (14.3) with equality,

(ii) all ℓ_1-realizations of $\square G$ are equicut of the form $\begin{pmatrix} A & O \\ J - A & J' \end{pmatrix}$ with $\lambda(d(G) + 1) - m$ columns, up to permutations of rows and columns, and taking complements of columns, where A is an ℓ_1-realization of G with scale λ.

Remark 14.3 $K_4 - P_3$, $K_4 - P_2$, the Dynkin diagram E_6 are examples of ℓ_1-graphs satisfying (14.1), (14.3), but not (14.2). *Affine* Dynkin diagram $\tilde{E}_6$ is an example of a graph that does not satisfy (14.1) and (14.3), but does satisfy (14.2).

Note that any graph G with diameter $D(G) = 2$ satisfies (14.1) and (14.2). Certainly, not all of them are ℓ_1-graphs, for instance, $K_{2,3}$. Also not all ℓ_1-graphs of diameter two satisfy (14.3), for instance, $K_{1,4}$.

In general, for any ℓ_1-graph $G = (V, E)$ with $|V| \geq 4$ one has

$$D(G) \leq s(d_G) \leq D(G) + |V| - 3. \tag{14.4}$$

The equality at the right-hand side of (14.4) holds if and only if G is a star, as can be seen by applying Theorem 1.1 of chapter 1.

Theorem 14.1 generalizes the situation for the cocktail-party graph $K_{n\times 2}$, considered in [DeLa97], chapter 7.4, to arbitrary ℓ_1-graphs. It implies, that the minimal scale of an ℓ_1-embedding of $\square G$ equals the minimal λ, such that the metric λd_G is embedded isometrically into H_m with $m = \lambda(D(G)+1)$. In particular case of $G = K_{4a}$, Lemma 7.4.6 of [DeLa97] gives for such a minimal λ, the inequality $\lambda \geq 2a$, with the equality if and only if there exists a Hadamard matrix of order $4a$.

Now we list many examples in no particular order. An equicut ℓ_1-graph is called a *doubling* if it is an antipodal doubling. Moreover, if it is obtained from a graph G_0 as in Theorem 14.1, we give such a representation $G = \square G_0$.

All equicut graphs with at most six vertices are: C_n $(2 \leq n \leq 6)$, K_n, $(n = 4, 5, 6)$, P_3, 4-wheel and the octahedron $K_{3\times 2}$. Amongst these eleven graphs only K_n is not ℓ_1-rigid and only C_4, C_6 and $K_{3\times 2}$ are doublings.

The scale of the direct product $G \times G'$ of two l_1-graphs is the least common multiple of the scales of G and G', and the size will be the sum of their sizes. Moreover, $G \times G'$ is ℓ_1-rigid if and only if G and G' are.

Lemma 14.5 *If l_1-graphs G, G' have even number of vertices each, then $G \times G'$ is an equicut graph if and only if they are.*

A *Doob graph* (the direct product of a number of copies of *Shrikhande graph* and a number of copies of K_4 (see, for example, [BCN89], page 27) is an example of an equicut graph obtained via Lemma 14.5. It is a (non ℓ_1-rigid and non-doubling) ℓ_1-graph of scale two.

Embeddable distance-regular graphs.

Here we again freely use notation from [BCN89]; also, a significant use is made of [KoSp94].

A graph of diameter d is called *distance-transitive graph*, if it is connected and admits a group of automorphisms, which is transitive, for any $1 \leq i \leq d$, on the set of all pairs of its vertices, being on the distance i. More general, a connected graph is called *distance-regular graph*, if it is regular and, given two vertices x and y, the number of vertices at distance i from x and at distance j from y depends only on the distance d(x,y).

Any distance-regular graph of diameter two is called *strongly regular graph*. All hypermetric polytopal strongly regular graphs are:

- $(n \times n)$-grids $K_n \times K_n$,

- triangular graphs $T(n) = J(n, 2)$,
- the skeleton $K_{n\times 2}$ of β_n,
- $G(1_{21}) = \frac{1}{2}H_5$ and
- $G(2_{21})$=the Schläfli graph;

only the last one, the Schläfli graph, is not ℓ_1-embeddable.

Reference [Kool90] proved that all finite distance-regular graphs, embeddable with scale one into an H_m are the distance-transitive ones:

- γ_m,
- C_{2m} and
- for odd m, Double Odd graphs DO_m.

In [KoSp94] all ℓ_1-embeddable distance-regular finite graphs are found.

Moreover, the Petersen graph and the Shrikhande graph are both equicut graphs of scale two and size 3; both are ℓ_1-rigid and are not doublings. The Double Odd graph DO_{2s+1} is an equicut graph of scale one and size $2s + 1$. The halved cube $\frac{1}{2}H_m$ is an equicut graph of scale two and size m. It is not ℓ_1-rigid only for $m = 3, 4$; it is a doubling if and only if m is even. The Johnson graph $J(2s, s)$ is a non ℓ_1-rigid doubling of scale two and size s.

Further, the following graphs are distance-regular equicut graphs.

(1) Any Taylor ℓ_1-graph: $\frac{1}{2}H_6$, $J(6, 3)$, C_6, H_3, icosahedron. They are all doublings of diameter three and size 3; they can be constructed using Theorem 14.1 above.
(2) Any strongly regular ℓ_1-graph, except $J(s, 2)$ $(s \geq 5)$ and any $(s \times s)$-grid $H(2, s)$ with s odd. That is, C_5, the Petersen graph, $\frac{1}{2}H_5$, the Shrikhande graph, H_m with m even, $K_{s\times 2}$.
(3) Amongst distance-regular graphs G with diameter greater than two and $\mu > 1$: $\frac{1}{2}H_m$ with $m > 5$, $H(m, d)$, $J(s, t)$ with $t > 2$, icosahedron and Doob graphs.
(4) All Coxeter ℓ_1-graphs except $J(s, t)$ with $t < \frac{s}{2}$: $J(2s, s)$, icosahedron, dodecahedron, $K_{s\times 2}$, $\frac{1}{2}H_s$, H_s, C_s $(s \geq 5)$.
(5) All cubic distance-regular ℓ_1-graphs: K_4, Petersen graph, H_3, DO_5, dodecahedron.

Also all amply-regular ℓ_1-graphs with $\mu > 1$ are equicut graphs. Yet another example is given by the 12-vertex co-edge regular subgraph of the Clebsh graph $\frac{1}{2}H_5$, (see [BCN89], chapter 3.11, page 104). It is an equicut

graph of size $\frac{5}{2}$, scale two, non-doubling.

Reference [Macp82] showed that any *infinite distance-transitive graph* G of *finite* degree arises in the following way: the vertices of G are p-valent vertices of T, two of them being adjacent if they lie at distance two in T, where T is an infinite tree, in which the vertices of the bipartite blocks have degrees p, q, respectively. (In other words, G is the halved subgraph of the infinite distance-biregular tree T.) The graph induced by all neighbors of fixed vertex of G, is the disjoint union of p complete graphs K_{q-1}. It is easy to see that, in general, $G \to \frac{1}{2}Z_\infty$. In the special case $q = 2$, it is just the infinite p-regular tree and it is embedded into Z_∞, except the case $p = q = 2$, when it is the infinite path $P_Z \to Z_1$.

Some equicut graphs, which are doublings of ℓ_1-graphs (see some in chapter 7.2 of [DeLa97]).

(1) $C_{2s} = \square P_s$.
(2) $K_{s\times 2} = \square K_s$.
(3) $H_s = \square H_{s-1}$.
(4) $J(2s, s) = \square J(2s-1, s)$.
(5) $\frac{1}{2}H_{2s} = \square \frac{1}{2}H_{2s-1}$.
(6) $Prism_{2s} = \square C_{2s}$
(7) $APrism_{2s+1} = \square C_{2s+1}$.
(8) Do is the doubling of $C_{\{1,2,\ldots,9\}}$ with an extra vertex connected to the vertices 3, 6 and 9 of the circle.
(9) Ico is the doubling of a 5-wheel; as well, it is the doubling of the graph obtained from hexagon $C_{\{1,2,\ldots,6\}}$ by adding edges (2,4), (2,6) and (4,6).
(10) $J(6, 3)$ is the doubling of the Petersen graph, in addition to the 4th item above for $s = 3$.
(11) $\frac{1}{2}H_6$ is the doubling of the Shrikhande graph and of (4×4)-grid $H_{2\times 4}$ (more precisely, of its realization in $\frac{1}{2}H_6$), in addition to the 5th item above for $s = 3$.

In the items 9, 10, 11, we have (diametral) switching-equivalent graphs G, such that $\square G$ is a Taylor ℓ_1-graph; see the definition preceding Theorem 14.1. This situation, in general, is well-known. For instance, the Gosset graph (it is a Taylor graph, which is not an ℓ_1-graph) can be obtained as the diametral doubling of one of five non-isomorphic, but switching-equivalent, graphs. For definitions and discussion of this situation in more general setting see, for example, [BCN89], pages 103–105.

Equicut polytopes.

The skeletons of many "nice" polytopes are equicut graphs. Below we list several such examples.

All five Platonic solids have equicut skeletons; all, except the tetrahedron α_3, are ℓ_1-rigid. All except the cube γ_3 (of scale one) have scale two. The sizes for α_3, β_3, γ_3, Ico and Do are $\frac{3}{2}$, 2, 3, 3 and 5, respectively.

The skeleton of any zonotope is a doubling, and it has scale one; so, it is ℓ_1-rigid.

Amongst all ℓ_1-embeddable semi-regular polyhedra, we have:

(1) all zonohedra (i.e. 3-dimensional zonotopes) are as follows: the truncated octahedron, the truncated cuboctahedron, the truncated icosidodecahedron and $Prism_{2s}$ ($s > 2$) with sizes 6, 9, 15 and $s + 1$, respectively;
(2) all other doublings are as follows: the rhombicuboctahedron, the rhombicosidodecahedron and $APrism_{2s+1}$ ($s > 1$) with scale two and sizes 5, 8 and $s + 1$, respectively;
(3) all remaining equicut polytopes are: the snub cube, the snub dodecahedron and $APrism_{2s}$ ($s > 1$); all have scale two and sizes $\frac{9}{2}$, $\frac{15}{2}$ and $s + \frac{1}{2}$, respectively;
(4) the remaining $Prism_{2s+1}$ ($s > 1$) has scale two and size $s + \frac{3}{2}$; it is not an equicut graph.

Amongst all Catalan (dual Archimedean) ℓ_1-embeddable polyhedra we have:

(1) all zonohedra are as follows: dual cuboctahedron and dual icosidodecahedron of sizes 4 and 6, respectively;
(2) the only other doubling is dual truncated Ico of scale two and size 5;
(3) all remaining cases (duals of tr(γ_3), tr(Do), tr(α_3) and $Prism_3$) are non-equicut ℓ_1-graphs of scale two and sizes 6, 13, $\frac{7}{2}$ and 2, respectively.

All Platonic, semi-regular and dual to semi-regular ℓ_1-polyhedra are ℓ_1-rigid, except the tetrahedron and the dual $Prism_3$. All *not* equicut graphs amongst them (see the columns "cuts" in Tables 4.1, 4.2) are: $Prism_n$ for odd n and duals of four semi-regular polyhedra ($Prism_3$ and truncated ones of tetrahedron, cube, dodecahedron).

Examples of regular-faced polyhedra (from the list of 92 polyhedra) with equicut skeletons (all have scale two) are: Nr.75 (biaugmented $Prism_6$) of

size 4 (a doubling) and two non-doublings: Nr.74 (augmented $Prism_6$) of size 4 and Nr.83 (tridiminished Ico) of size 3.

The regular ℓ_1-embeddable polytopes of dimension greater than three, have equicut skeletons. They are as follows: α_n, γ_n and β_n.

There are just three semi-regular ℓ_1-embeddable polytopes of dimension greater than three (see [DeSh96]). Two of them have equicut skeletons: $\frac{1}{2}H_5$ and the snub 24-cell. The latter is a 4-dimensional semi-regular polytope with 96 vertices. The regular 4-polytope 600-cell can be obtained by capping its 24 icosahedral facets. Its skeleton has scale two and size six; it is a doubling.

Three of the chamfered Platonic solids have ℓ_1-skeletons: Cham(γ_3) is a zonohedron of size 7, Cham(Do) has an equicut (non-doubling) skeleton of scale two and size 11, Cham(α_3) has non-equicut ℓ_1-skeleton of scale two and size 4.

14.2 Scale one embedding

Remind first (see chapter 1) that a finite ℓ_1-graph is embeddable with scale one if and only if it is bipartite and 5-gonal.

Small bipartite polyhedral graphs

Amongst six bipartite polyhedral graphs with at most nine faces, there are two embeddable ones, the cube 4_8 and the $4_{12} = Prism_6$; both are zonohedra, embeddable in H_3 and H_4, respectively. Other four are the oc_8^*, oc_9^*, 4_{14} and the not 5-gonal 12-vertex graph on Figure 14.2 a). Amongst five bipartite polyhedral graphs with ten faces and at most 13 vertices, there are two embeddable ones, a oc_{10}^* and $RhDo$-v_3 (see Figure 14.2 c) and d); they are also Nr.13 (for t=1) and 2 in Table 14.1. Other three are the second oc_{10}^*, the $APrism_5^*$ and the not 5-gonal 13-vertex graph on Figure 14.2 b). Both above embeddable graphs are embedded into H_4, but only the graph on Figure 14.2 d) is not centrally symmetric. Remind that we allocate to polyhedra, presented only by their combinatorial type, the maximal possible symmetry. For example, the graph on Figure 14.2 c) and, in general, any polyhedron $C_4 \times P_{t+2}$, $t \geq 1$ from Table 14.1 is seen as a centrally-symmetric one, but it is not zonotope, since it should have some trapezoidal faces in order to be realisable as a convex polyhedron.

A *non-convex* realization of $C_4 \times P_3$ (as two adjacent cubes) tiles the 3-space *non-normally*; see the partition Nr.35 in Table 10.3) and the graph

of this tiling is embedded into Z_3. Nr.15–16 of Table 14.1 are Voronoi t-polytopes for the lattices Z_t and A_t^*; the polyhedra Nr.1, 3 and 4 are Voronoi polyhedra of the lattices $A_2 \times Z_1$, A_3 and L_5 (see chapter 11).

Recall that Nr.2 of Table 14.1 ($RhDo$-v_3, i.e. $RhDo$ with a deleted simple vertex) is the tile of three Voronoi partitions from Tables 10.1, 10.2 and 10.3: Nr.25, which is embeddable into Z_4, and not 5-gonal ones Nr.26 and 33. Apropos, two 13-vertex graphs on Figure 14.2 b) and d), are exactly two smallest non-Hamiltonian bipartite polyhedral graphs, which can be realized as the Delaunay tesselation of their vertices (see Figure 10 in [Dill96]).

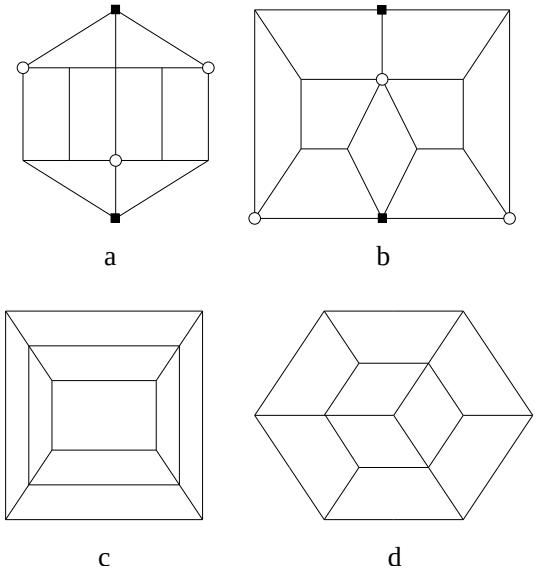

Fig. 14.2 **Some small bipartite polyhedral graphs**

Zonotopes

Zonotopes are affine projections (called *shadows* in [Coxe73]) of hypercubes γ_m. (Apropos, any convex polytope is affine projection of a simplex α_m and any centrally symmetric convex polytope is affine projection of a cross-polytope β_m.)

Remind that a dicing can be seen as a lattice, the Voronoi polytope of which is a zonotope (see [Erda98]).

The following result was proved in [BEZ90].

Proposition 14.1 *The skeleton of any zonotope of diameter m is isometrically embeddable into the skeleton H_m of γ_m, whose affine projection it is.*

Remark 14.4 Examples of zonotopes are:

(1) five of Archimedean and their dual (Catalan) polyhedra are zonohedra: Nr.5, 9, 11 and 3, 6 of Table 14.1;
(2) All five (combinatorially different) Voronoi polyhedra are zonohedra: cube $\gamma_3 = H_3$, rhombic dodecahedron RhDo $\rightarrow H_4$, $Prism_6 \rightarrow H_4$, elongated dodecahedron ElDo $\rightarrow H_5$, truncated $\beta_3 \rightarrow H_6$;
(3) All five *golden isozonohedra* of Coxeter (zonohedra with all faces being rhombic with the diagonals in golden proportion) are:
2 types of hexahedra (equivalent to γ_3), rhombic dodecahedron, rhombic icosahedron $Pz(5)$ and triacontahedron (i.e. dual icosidodecahedron).
(4) Curious family of eight 3-zonotopes, embeddabble into H_m, $3 \leq m \leq 10$, and having $m(m-1)$ faces, is given in [ScYo00].
(5) Besides $Prism_{2m}$ and γ_m, some examples of infinite families of zonotopes (Nr.12–16 in Table 14.1) are polar zonohedra $Pz(m) \rightarrow H_m$ (γ_3, RhDo, rhombic icosahedron for $m = 3, 4, 5$, respectively, see [Coxe73]) and m-dimensional permutahedra (for $m = 2$ and 3, it is C_6 and truncated β_3, respectively).

The tope graphs of oriented matroids

An *oriented matroid* on E is a pair $M = (E, \mathbf{F})$, where E is a finite (m-element) set and $\mathbf{F}$ is a set *sign vectors* on E (called *faces*), which satisfy some special axioms (see, for example, [Fuku95]). A natural order on signed vectors (on E) defines the *rank of a face f* as the length of any maximal chain from 0 to f. The maximal faces are called *topes*; the common rank r of topes is called the *rank of the oriented matroid M*. The *top graph* of M is the graph, denoted by $T(M)$, having the topes as vertices, with two of them being adjacent if they have a common face of rank $r-1$. The tope graph uniquely defines the oriented matroid.

A graph is called *antipodal*, if for each its vertex a there is an unique vertex a' such that a' has larger distance from a than any of neighbors of a'. If the skeleton of a polytope is antipodal, then the maximal symmetry of this polytope contains central symmetry. In those terms, the following results by Fukuda and Handa (see [Fuku95]) connects isometric subgraphs of hypercubes with above tope graphs of an oriented matroids $M = (E, \mathbf{F})$

Table 14.1 **Some isometric polyhedral subgraphs of hypercubes**

Nr.	Nr. vertices	deg.	polyhedron	emb. in	Aut	zonotope?
1	12	3	$Prism_6$	H_4	D_{6h}	+
2	13	3,4	$RhDo - v_3$	H_4	C_{3v}	non-CS
3	14	4	$(cuboct.)^* = RhDo$	H_4	O_h	+
4	18	3,4	ElDo	H_5	D_{4h}	+
5	24	3	tr(β_3)	H_6	O_h	+
6	32	4	$(icosidode.)^* = triac.$	H_6	I_h	+
7	32	3	Cham(γ_3)	H_7	O_h	+
8	32	3	$tw.$ Cham(γ_3)	H_7	D_{3h}	non-CS
9	48	3	tr(cuboct.)	H_9	O_h	+
10	56	3,4	Fukuda's polyhed.	H_9	C_i	no
11	120	3	tr(icosidode.)	H_{15}	I_h	+
12	$4t > 12$	3	$Prism_{2t} = C_{2t} \times P_2$	H_{t+1}	D_{2th}	+
13	$4(t+2) > 8$	4	$C_4 \times P_{t+2}$	H_{t+3}	D_{4h}	no
14a	$t(t-1)+2$	3, $t > 4$	$Pz(t)$, $t > 3$ odd	H_t	D_{td}	+
14b	$t(t-1)+2$	3, $t > 4$	$Pz(t)$, $t > 4$ even	H_t	D_{th}	+
15	2^t	t	t-hypercube	H_t		+
16	$(t+1)!$	t	permutahedron	$H_{\binom{t+1}{2}}$		+

of rank $r \geq 3$ on m-element set E:

(i) $T(M)$ is an r-connected antipodal graph and $T(M) \to H_m$;

(ii) A graph is the top graph of an oriented matroid of rank three on m-element set if and only if it is the skeleton of a centrally symmetric polyhedron, which is isometric subgraph of H_m.

If $T(M)$ is the skeleton of a zonotope, then this zonotope is r-dimensional and has diameter m. We are interested now by construction of non-zonotopal centrally-symmetric polyhedra.

Every Voronoi polytope is centrally symmetric with centrally symmetric facets. But a zonotope additionally has centrally symmetric faces of all dimensions. The skeleton $G(P)$ of a zonotope P is the *top graph* of an oriented matroid $M(P)$, which is *realized* by the zonotope P. Hence such oriented matroid is called *realizable oriented matroid*, or *linear* one. A face of dimension k of P realizes an oriented matroid of rank k.

Consider a 3-dimensional zonotope, i.e. a zonohedron P. Let F and F' be two opposite faces of P. Let F has $2k$ edges, $k \geq 3$. These edges are parallel to k vectors. These k vectors are linearly independent and form a circuit $C(F)$ of the matroid $M(P)$. Let $\{(i, i') : 1 \leq i \leq 2k\}$ be $2k$ pairs of antipodal vertices of F and F', respectively. Denote by $Q(G)$ the graph

obtained from $G := G(P)$ by adding two new vertices v, v' and new edges (v, i), (v', i') for $i = 2j + 1$, $0 \le j \le k - 1$. Clearly, $Q(G)$ is antipodal and G is an isometric subgraph of $Q(G)$. If $G \to H_m$, then $Q(G) \to H_m$ also. (In fact, let $a(1) = \emptyset$, $a(2j+1) = \{1, j+1\}$, $1 \le j \le k-1$; then $a(v) = \{1\}$ is uniquely determined.)

If G is a 3-connected planar graph, then so, is $Q(G)$. Hence $Q(G)$ is the skeleton of a polyhedron, which we denote by $Q(P)$. It is centrally symmetric. Usually, if P is a zonohedron, so is $Q(P)$. But now, the set of vectors, representing F and F', is not a circuit of the oriented matroid $M(Q(P))$.

Consider elongated dodecahedron ElDo and rhombic dodecahedron RhDo. One can check, that $Q(Prism_6)$ is $RhDo$, $Q^2(ElDo)$ is the rhombic icosahedron $Pz(5)$, $Q^4(\mathrm{tr}(\beta_3))$ is the triacontahedron, i.e. dual icosidodecahedron. (Here $Q^m(P) := Q(Q^{m-1}(P))$.)

But there are cases, when the polyhedron $Q(P)$ is not a zonohedron and hence, it does not realizes an oriented matroid. An example was given by Fukuda in [Fuku95] (using a hexagonal faces F and F', on which new vertices were put); see Figure 14.3.

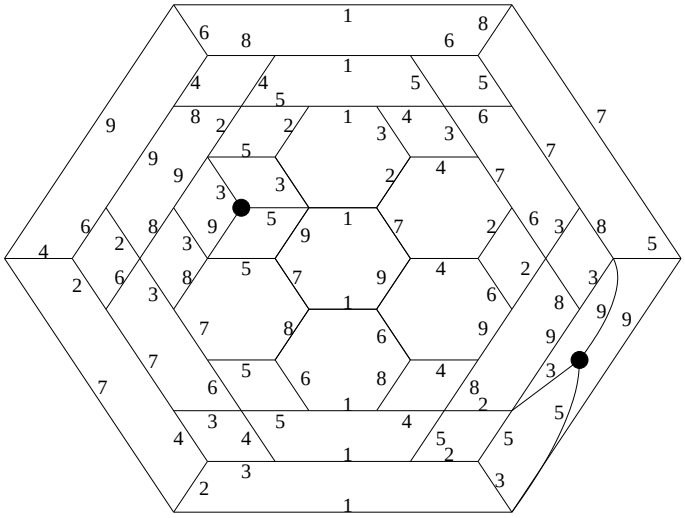

Fig. 14.3 **A non-zonotopal centrally symmetric polyhedron, whose skeleton is embeddable into H_9**

This polyhedron contains 56 vertices, 18 hexagonal and 18 square faces. It is an example of a non-zonotopal centrally symmetric polyhedron, whose

skeleton is embedded into H_9. This polyhedron is a minimal one in the following sense: any centrally symmetric 3-polytopal isometric subgraph of H_m, $m \leq 8$, is (being the tope graph of an rank-three oriented matroid with at most eight elements) the skeleton of a zonotope.

Fukuda constructed it as (non-Pappus) extension of an oriented rank-three matroid on eight points. As a *linear* extension of the same matroid, he obtain a dual zonohedron of diameter nine, having 54 vertices, 20 hexagonal and 12 square faces: just delete two marked opposite vertices from 56-vertex polyhedron depicted in Figure 14.3 above.

Remark 14.5 See [DeSt96; DeSt97] for similar isometric embeddings of skeletons of *infinite* polyhedra (plane tilings) into cubic lattices Z_n. For example, regular square tiling regular and hexagonal tiling are embeddable into Z_2 and Z_3; they are Voronoi partitions of the lattices Z_2, A_2. The Archimedean tilings (4.8.8), (4.6.12) and dual Archimedean tiling [3.6.3.6] are embeddable into Z_4, Z_6, Z_3. Also Penrose aperiodic rhombic tiling is embeddable into Z_5 and dual mosaic Nr.12 (from Table 9.1 above) is embeddable into Z_∞. The tiling on Figure 14.4 b embeds also into Z_∞. Clearly, any *lattice plane* tiling, such that its Voronoi partition is embeddable into a Z_m, is a dicing. In other words, it is *zonohedral*, i.e. having only centrally symmetric faces. Any zonohedral plane tiling embeds into a $Z_m, m \leq \infty$. A zonohedral plane tiling needs not to be periodic (for example, Penrose aperiodic tiling by two golden rhombuses) or to be a projection of Z_m, $m < \infty$ (see, for example, the tiling on Figure 14.4 a). The tiling [3.6.3.6] above is non-zonohedral, since its quadrangular faces are not centrally symmetric.

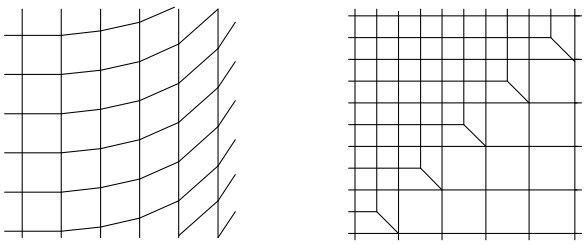

Fig. 14.4 **Two embeddable tilings**

Some generalizations of planar scale 1 embeddable graphs

Let G be a bipartite plane graph. If it is infinite, we suppose that its vertices have bounded degree and that it is *discrete*, i.e. any ϵ-neighborhood of any point on the plane contains only finite number of its vertices. Call such a graph G *admissible* (or *strictly admissible*) if there exist a mapping f of its vertices into vertices of an hypercube H_m, $m \leq \infty$, such that its edges (x, y) are mapped into edges $(f(x), f(y))$ of H_m and the images of the circuits, bounding its interior (or, respectively, all) faces are isometric subgraphs of the same H_m. Using a result from [DSS86], we have that G is admissible (or strictly admissible) if and only if every of its zone (i.e. non-extendible sequence of opposite edges) is simple, i.e. it has no self-intersections. (In strictly admissible case the exterior face is included; so, G is considered as a graph on the sphere and zones can go through the exterior face.) In fact, if a zone self-intersects in a face, then the circuit, bounding this face, will be not isometric in H_m. On the other hand, if G is a plane *quadriliage*, i.e. all its interior faces are 4-gons, then it was proved in [DSS86] that it is admissible (or strictly admissible) if and only if all its zones are simple. The general case of admissible (or strictly admissible) graph G can be reduced to above one by partition of all interior (or, respectively, all) faces into 4-gons; so that the zones and their simplicity (or not) are preserved.

In terms of zones, we have that G is scale one embeddable (i.e. an isometric planar subgraph of a hypercube) if and only if it is admissible and, moreover, every its zone is convex. In fact, zones are belts, corresponding to convex opposite cuts, such that exactly one of them goes through any edge.

A partial subgraph of an hypercube is always bipartite; its vertices are mapped *injectively* into those of the hypercube. Clearly, there are following irreversible implications for possible properties of graphs with respect to the hypercubes:

isometric (i.e. scale 1 embeddable) $\rightarrow$ induced $\rightarrow$ partial $\rightarrow$ bipartite,

isometric planar $\rightarrow$ admissible $\rightarrow$ bipartite planar. (We take for each graph its strongest property; for example, the 8-cycle, which is only a partial subgraph of H_3, is considered isometric since it is isometric subgraph of H_4.)

On Figure 14.5 we have seven counterexamples. In the last graph g), two vertices, marked by a black circle, are the points of self-tangency of the zones of eight 4-gons around them; the images of two vertices, marked by a white circles, coincide in H_6.

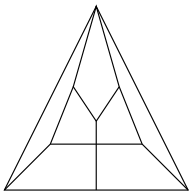

a) the dual of $APrism_4$ is bipartite planar, but non-admissible and non-partial one

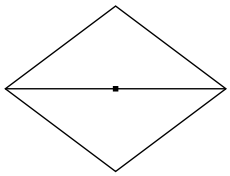

b) $K_{2,3}$ is admissible in H_2, but non-partial

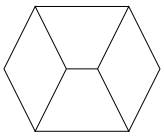

c) the cube with deleted edge is admissible and partial in H_3, but non-induced

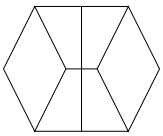

d) admissible and induced in H_4, but non-isometric

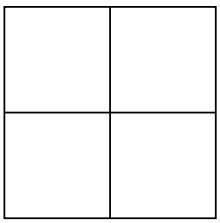

e) isometric, but not strictly admissible

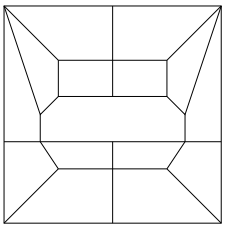

f) induced in H_6, but not admissible

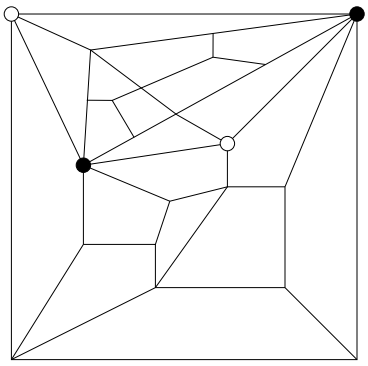

g) strictly admissible in H_6, but non-partial

Fig. 14.5 **Seven counterexamples**

Chapter 15

Some Generalization of ℓ_1-embedding

15.1 Quasi-embedding

Here we consider *quasi-embedding* or, more exactly, *t-embedding* of given graph G, i.e. our usual embedding, but for *t-truncated distance* $min(t, d_G)$, where t is less than the diameter of the graph G. We say that a metric d is *t-embeddable* if there is an ℓ_1-embeddable metric d' such that $d'_{i,j} = min(d_{i,j}, t)$. This notion was introduced in [DeSh96], where it was shown that the polynomial algorithm given there for the recognition of ℓ_1-graphs can be extended to the recognition of t-embeddable graphs.

In what follows, describing a t-embedding of a polyhedron P, we associate to every its vertex v a subset $a(v)$ of a set N. Usually we take as N the set of all faces, which are k-gons for a fixed k. We say that a face F is *reachable* by an m-path from a vertex v if there is an m-path of length m from the vertex v to a vertex of the face F. We use here notation C_{60} for the truncated icosahedron $5_{60}(I_h)$. Even if C_{60} is not ℓ_1-embeddable, we still can *quasi*-embed it into $\frac{1}{2}H_{20}$ in the following sense.

According to [DeSh96], the truncated icosahedron (of diameter 9) has a *unique* 7-embedding into $\frac{1}{2}H_{20}$: associate each vertex to 2+2+3 hexagons (amongst all 20) reachable by 0-, 1-, 2-paths, respectively. It is also the unique 3-embedding, but not unique 2-embedding: for example, associate every vertex to two its hexagons. The unique 3-embedding of C_{60} into $\frac{1}{2}H_{20}$ is called *quasi-*C_{60}. Moreover, quasi-C_{60} is an ℓ_1-rigid (but not graphic) metric.

The Figure 15.1 illustrates the 7-embedding of C_{60}. The construction is as follows: we can associate a coordinate of $\mathbb{R}^{20}$ to each of the 20 hexagons. Then a vertex v (for example the white atom of Figure 15.1) is mapped into the vertex $\phi(v)$ of the half-cube $\frac{1}{2}H_{20}$ (in odd representation), whose

non-zero coordinates correspond to the seven hexagons of C_{60} containing a vertex, whose distance to v is less than three (the seven grey hexagons of Figure 15.1). This give us a 7-embedding of C_{60} into the half-cube $\frac{1}{2}H_{20}$. All distances eight and nine in C_{60} became seven in quasi-C_{60} (recall that C_{60} has diameter 9).

The automorphism group of quasi-C_{60} (i.e. all permutations of the 20 coordinates indexed by the 20 hexagons of C_{60}, which preserve quasi-C_{60}) is equal to the one of C_{60}, which is the Coxeter group H_3 isomorphic to $\{1,-1\} \times A_5$. The Figure 15.2 illustrates one automorphism of quasi-C_{60}: the reversing of the spiral Hamiltonian path on the 20 hexagons of C_{60}.

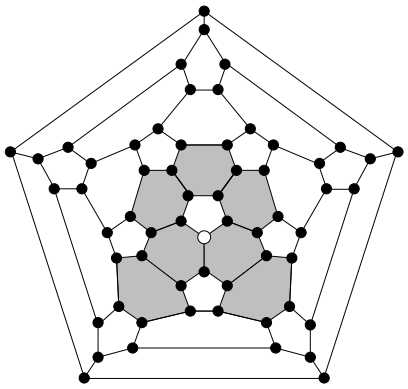

Fig. 15.1 **Embedding up do distance 7 of $C_{60}(I_h)$ into $\frac{1}{2}H_{20}$**

Icosidodecahedron (of diameter 5) has *unique* ([DeSh96]) 4-embedding in $\frac{1}{2}H_{12}$: associate every vertex to 1+1+2 pentagons (from all 12) reachable by 0-, 1-, 2-paths. It is also a unique 3-embedding, but there is another 2-embedding: associate every vertex to two its triangular faces.

Cuboctahedron (of diameter 3) has at least two following 2-embeddings:

into $\frac{1}{2}H_6$: associate every vertex to its two square faces,

into $\frac{1}{2}H_8$: associate every vertex to its two triangular faces; this one, as well as two above ones are t-embeddings into $\frac{1}{2}H_{2d(P)+2}$, where $d(P)$ is the diameter of P.

The vertex figure (and the local graph of the skeleton) of the snub 24-cell is the tridiminished icosahedron (the regular-faced solid $M_7 = Nr.\,83$ of diameter 3). It is embedded into $\frac{1}{2}H_6$ and has a 2-embedding into $\frac{1}{2}H_7$.

Any simple polyhedron has a 2-embedding in the tetrahedral graph

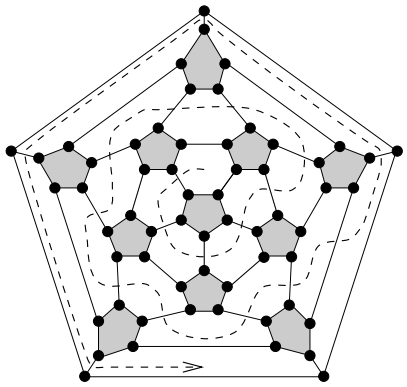

Fig. 15.2 **The spiral Hamiltonian automorphism of quasi-C_{60}**

$J(n,3)$ (so in $\frac{1}{2}H_n$): associate every vertex to its three faces. If the diameter of a simple polyhedron is at least 3, then it is 3-embeddable if and only if sizes of its faces are from the set $\{3,4,5\}$. Examples of this procedure are:

(1) dodecahedron (of diameter 5) has a 3-embedding into Johnson graph $J(12,3)$; also it has a 5-embedding into $\frac{1}{2}H_{10}$,
(2) $\alpha_3 \to J(4,3) \to \frac{1}{2}H_4$ (not unique),
(3) $M_{25}^* \to J(8,3) \to \frac{1}{2}H_8$,
(4) a 2-embedding of $Prism_n$, which turns out to be $Prism_n \to \frac{1}{2}H_{n+2}$ ($\to H_{\frac{n+2}{2}}$ for even n).

Another procedure: fix a 5-wheel ∇C_5 in the skeleton of an icosahedron and associate every vertex v to the set of all vertices of the 5-wheel at distances 0 and 1 from v; we get the (unique) 3-embedding of the icosahedron.

The dual of $F_{60}(C_s)_r$, considered on Figure 22 of [DDG98], admits a 4-embedding into $\frac{1}{2}H_{10}$. More precisely, $F_{60}^*(C_s)_r$ has diameter 5 and all distances are preserved except those between four opposite pentagons: $(\overline{38},48)$, $(\overline{1378},1478)$, $(\overline{45},35)$ and $(\overline{2459},2359)$. Instead of five, those distances became four in $\frac{1}{2}H_{10}$. See Figure 15.3, where the 4-embedding of $F_{60}^*(C_s)_r$ is given by labels of facets of $F_{60}(C_s)_r$. Additionally, a not 5-gonal configuration of $F_{60}(C_s)_r$ is given, in Figure 15.3.

The following Theorem (see [DFS03]) describe completely t-embeddings for fully icosahedral (i.e. with symmetry I_h) fullerenes and their duals.

Theorem 15.1

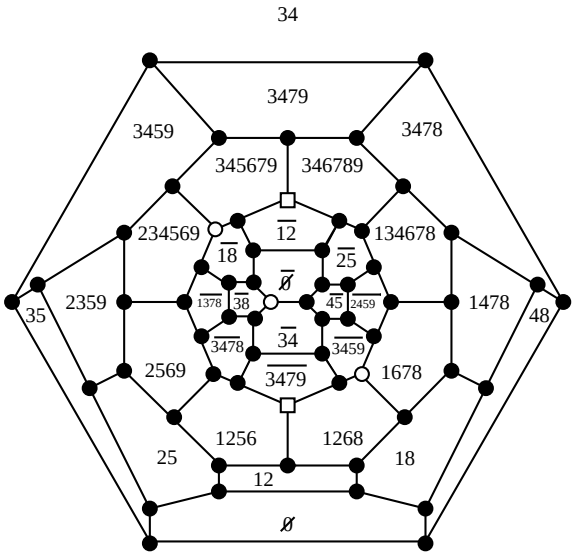

Fig. 15.3 **The 4-embedding of $F^*_{60}(C_s)_r$ into $\frac{1}{2}H_{10}$ and a not 5-gonal configuration of $F_{60}(C_s)_r$**

(i) $C_{20k^2}(I_h)$, $k \geq 1$, *is* $(2k+7)$*-embeddable into* $\frac{1}{2}H_{12k-2}$*; its diameter is* $6k-1$,

(i') $(C_{20k^2}(I_h))^*$, $k \geq 2$, *is* $2k$*-embeddable into* $\frac{1}{2}H_{6k}$*; its diameter is* $3k$,

(ii) $C_{60k^2}(I_h)$, $k \geq 1$, *is* $(6k+1)$*-embeddable into* $\frac{1}{2}H_{20k}$*; its diameter is* $10k-1$,

(ii') $(C_{60k^2}(I_h))^*$, $k \geq 1$, *is* $(3k+2)$*-embeddable into* $\frac{1}{2}H_{10k}$*; its diameter is* $5k$.

In fact, let us indicate for each of four above cases, the complete collection of zones, giving a t-embedding. Each zone will be without self-intersections; so any two of them will be either *parallel*, i.e. disjoint, or intersect exactly in two faces. We call a zone of faces of a fullerene *special* or *pure*, according to if it contains or no some pentagons. The dimension of the half-cube is the number of special zones plus twice the number of pure ones. This dimension turns out to be twice the diameter of the graph in the cases (i), (i') and (ii'). Remark that this t-embedding is isometric only for $k = 1$ in the cases (i), (i'), (ii') and for $k = 2$ in the case (i). In the case (i') above there are $6k$ alternating zones of length $10k$ each; they are partitioned

into six parallel classes. In the case (ii') above there are $10k$ alternating zones of length $18k$ each; they are partitioned into ten parallel classes. In the case (i) above there are $6(k-1)$ pure zones of length $5k$ each; they are partitioned into six parallel classes; there are ten special (alternating) zones of length $6k$ each. Each special zone consists of six pentagons, separated by $(k-1)$-strings of hexagons. Each zone have equal number (six for pure and three for special one) of pentagons inside and outside of it. In the case (ii) above there are $10(k-1)$ pure zones of length $9k$ each; there are 20 special (alternating) zones of length $9k$ each. Each special zone is not alternating; it consists of three pentagons, separated by $(3k-1)$-strings of hexagons. Each pure zone have six pentagons inside and outside of the ring formed by the zone; each special one has exactly three pentagons inside or outside of it. All $20k$ zones are partitioned into ten parallel classes and each class consists of $k-1$ pure zones, taken in a "sandwich" by two special ones.

15.2 Lipschitz embedding

Here we consider another relaxation of our main notion of l_1-embedding. The mapping $f : X \to Y$ of metric spaces X, Y is called *Lipschitz*, if for any vertices a, b of X, holds

$$1 \leq \frac{d_X(a,b)}{d_Y(f(a),f(b))} \leq C,$$

where C is a constant, called *distortion*. Bourgain showed in 1985 that any metric on at most n points is Lipschitz-embeddable into ℓ_1^k (for a finite dimension k) with distortion $C = O(log\, n)$; Linial, London and Rabinovitch showed in 1994 that, moreover, $k = O((log\, n)^2)$. For example, $K_{1,3}$ has distortion > 1. Aharoni in 1978 showed that any l_p with $p > 2$ is not Lipschitz-embeddable into l_1.

It looks plausible that the path-metric of any infinite hypermetric graph (moreover, any 5-gonal metric) is Lipschitz-embeddable, up to a scale, into a Z_m, $m \leq \infty$.

15.3 Polytopal hypermetrics

The convex cone of all hypermetrics on m points is denoted by Hyp_m. Call a hypermetric d on m points *of rank* k, if the intersection of all faces of

Hyp_m, to which d belongs, has dimension k; call a hypermetric *extreme hypermetric*, if it has rank 1, i.e. it belongs to an extreme ray of Hyp_m.

A polytope $P \times P'$ is hypermetric if and only if both P, P' are hypermetric; it is non-embeddable if and only if at least one of P, P' is non-embeddable. (But, for example, any pyramid $Pyr(P)$ over polytope P with at least 28 vertices, is embeddable if and only if it is hypermetric.)

Any hypermetric, but not ℓ_1-embeddable graph of rank k has at most 56^k vertices; the skeleton of the direct product of k copies of the 7-dimensional Gosset polytope 3_{21} realizes equality in this upper bound.

We denote below by G_i, $1 \leq i \leq 26$, the graphs from [DeGr93] related (but not as path-metrics) to extreme hypermetric on seven points. Remark that extreme hypermetric graphs G_1 and G_2 are skeletons of 4-dimensional pyramids with bases Pyr_5 and 2-capped α_3, respectively.

All hypermetric but non-ℓ_1 *graphs* with at most seven vertices are known (see [DeGr93]); they are 12 graphic metrics amongst of 26 extreme hypermetrics on seven points.

Proposition 15.1 *Amongst of all hypermetric non-l_1 graphs with at most seven vertices, the polytopal ones are only: 3-polytopal G_4 (see Figure 15.4, d)) and 4-polytopal $G_1 = \nabla^2 C_5 = K_7 - C_5$, $G_2 = K_7 - P_4$.*

Any, except of K_2, hypermetric is extreme if and only if it generate 2_{21} or 3_{21}. So, the number of vertices of any extreme hypermetric graph is within the interval [7,56] and any polytope, such that its skeleton is extreme hypermetric, has dimension within the interval [6,7]. Call an extreme hypermetric graph of type I (of type II) if it generates the root lattice E_6 (E_7, respectively). A graph G of type I has diameter two, since it is an induced subgraph of the Schläfli graph $G(2_{21})$ of diameter two, and in this case ∇G is an extreme hypermetric of type II.

Clearly, $G(Pyr(P)) = \nabla G(P)$, $\dim(Pyr(P)) = \dim P + 1$. (Remark that $Pyr^k(C_5) \rightarrow \frac{1}{2}H_5$ for $k \in \{0, 1\}$, it is extreme hypermetric for $k \in \{2, 3\}$, and it is 7- but not 9-gonal for $k = 4$.)

Examples of polytopes, whose skeletons are extreme hypermetric but are not represented as $\nabla G'$ for an extreme hypermetric graph G' are:

of type I:

(1) the polyhedra Nr.30, 71, 106 $= M_{22}$ and one with skeleton G_4 all having 9, 9, 10 and 7 vertices, respectively (see Figure 15.4);
(2) the 4-polytopes with skeletons G_1, G_2 and both with seven vertices;
(3) the 6-polytopes: with skeletons $K_9 - C_6 = G(Pyr^3(Prism_3))$,

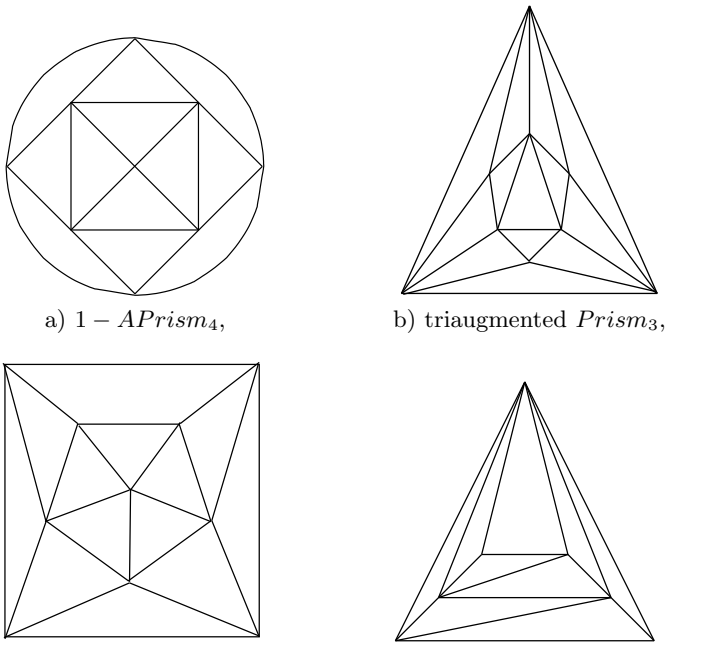

a) $1 - APrism_4$, b) triaugmented $Prism_3$,

c) sphenocorona M_{22}, d) extreme hypermetric graph G_4

Fig. 15.4 **Examples of hypermetric non-embeddable polyhedra**

$\nabla^2 T(5) = G(Pyr^2(\mathrm{Ambo}(\alpha_4)))$, $\nabla\frac{1}{2}H_5$ and the Shläfli polytope 2_{21} having, respectively, 9, 12, 17 and 27 vertices;

of type II:

(1) the polyhedra Nr.37, $107 = M_{21} + Pyr_4$
(2) and the 7-polytope 3_{21} with 10, 11 and 56 vertices, respectively.

So, we have two following series of inscribed polytopes, such that their skeletons are extreme hypermetrics:

$G_1 = \nabla^2 C_5 < \nabla^2 G(0_{21}) < \nabla G(1_{21}) < G(2_{21})$ (of type I),

$\nabla^3 C_5 < \nabla^3 G(0_{21}) < \nabla^2 G(1_{21}) < G(3_{21})$.

Some examples of extreme hypermetrics, which are not polytopal, but are close to polytopal in a sense:

(1) 7-vertex graph G_{18} of type I is a planar graph of a *skew* polyhedron.
(2) The skeleton of the stella octangula (the section of γ_3 by β_3 with vertices in the centers of faces of γ_3), which is a *non-convex* polyhedron; it is

14-vertex graph G_{so}. It contains the extreme hypermetric G_4 as an induced subgraph. G_{so} is an isometric subgraph of the Gosset graph $G(3_{21})$ and, since it has diameter 3, it is of type II.

(3) Antiwebs AW_9^2, AW_{12}^3, are of type I, and AW_{14}^3 is of type II; AW_9^2 is projectively-planar and it becomes planar, if we delete one edge.

Finally, one can enumerate isometric subgraphs (and polytopal ones between them) of a given half-cube $\frac{1}{2}H_n$, which are not isometric subgraphs of its facet. For example, the following graphs are such isometric polytopal subgraphs of the Clebsh graph $\frac{1}{2}H_5 = G(1_{21})$:

(1) C_5, $K_5 = G(\alpha_4)$ (together with four graphs from 2) below), they are only such subgraphs of $\frac{1}{2}H_5$ with at most 6 vertices);
(2) $K_6 - C_6 = G(Prism_3)$, $K_6 - P_5$ (polyhedral), $K_6 - P_4 = G(\text{2-capped } \alpha_3)$, $\nabla C_5 = G(Pyr_5)$ (amongst of all ten 6-vertex isometric subgraphs of $\frac{1}{2}H_5$);
(3) the skeletons of the following polyhedra with at least 7 vertices: Nr.27 (1-capped $Prism_3$), Nr.60 (augmented $Prism_3$), Nr.70 (biaugmented $Prism_3$), 1-capped β_3, $APrism_4$;
(4) the skeletons of 4-polytopes: $Pyr(Prism_3)$, $\alpha_1 \times \alpha_3$, $G(0_{21}) = T(5)$, $T(5) - K_1$, $T(5) - \overline{K_2}$, 1-capped (on a facet β_3) 0_{21};
(5) the skeletons of 5-polytopes: $Pyr^2(Prism_3)$, $Pyr(\text{ambo-}\alpha_4)$.

15.4 Simplicial n-manifolds

An interesting relaxation of our embeddings of polytopes is to consider scale-isometric embedding into hypercubes and cubic lattices of 1-skeletons of simplicial and cubical *complexes* more general than the boundary complexes of polytopes. For example, the simplicial complex on $\{1,2,3,4,5\}$ with the facets $\{1,2,3\}$, $\{1,2,4\}$, $\{1,2,5\}$ has the skeleton $K_5 - K_3$; the cubical complex on $\{1,2,3,4,5,6\}$ with the facets $\{1,2,3,4\}$, $\{2,3,5,6\}$, $\{1,4,5,6\}$ has the skeleton $K_{3,3}$. So, both are not 5-gonal.

While the general case of simplicial complexes is too vast, we have some partial results in terms of *links of $(n-2)$-faces*. For any n-simplex S containing fixed $(n-2)$-face S', there exists unique edge e, such that S is the join of S' and e. The *link of $(n-2)$-face S'* is the cycle formed by such edges e, for all n-simplexes S, containing S'.

Theorem 15.2 *Let M be a closed simplicial n-manifold of dimension $n \geq 3$. Then we have:*

(i) M is not embeddable, if it has an $(n-2)$-face belonging to at least five n-simplexes and such that its link is an isometric cycle in the skeleton.

(ii) M is embeddable, if any of its $(n-2)$-faces belongs to at most four (i.e. 3 or 4) n-simplexes.

If a $(n-2)$-face belongs to at least six n-simplexes (so, to at least six $(n-1)$-simplexes), then the skeleton of M is not 5-gonal, since it contains the isometric subgraph $K_5 - K_3$. For example, $De(A_3^*)$ is not 5-gonal, because it has six tetrahedra on some edges.

If a $(n-2)$-face belongs to exactly five n-simplexes, then the skeleton of M contains the isometric subgraph $K_7 - C_5$ (i.e., the skeleton of 4-polytope $Pyr(Pyr_5)$), which is 5-gonal but is not embeddable. For example, the regular 4-polytope 600-cell, which is a closed simplicial 3-manifold, has five tetrahedra on each edge.

The condition of isometricity of the link is necessary (it was missed in a result from [DeSt98]). For example, there exists an *embeddable* 3-manifold having an edge, which belongs to five tetrahedra; its skeleton is $K_7 - P_2$.

In order to check (ii) for $n = 3$, for example, consider closed simplicial 3-manifolds, such that any edge belongs to at most four tetrahedra. There are exactly five such manifolds. Their skeletons are $K_5 = G(\alpha_4)$, $K_{2\times 4} = G(\beta_4)$, K_6 (a 3-dimensional submanifold of α_5), $K_6 - e$, $K_7 - 2e$. All those five skeletons are embeddable into $\frac{1}{2}H_m$ with $m = 5, 4, 6, 8, 8$, respectively. One can show, that the skeleton of any n-manifold in the case (ii) is the graph $K_i - tP_2$ (i.e. the i-clique with t disjoint edges deleted), such that either $(i, t) = (2n + 2, n + 1)$, or

$n \geq t + 1$ and $n + t + 2 \leq i \leq n + t + 1 + \lfloor \frac{n-t+1}{2} \rfloor$.

In fact, any subgraph of the skeleton of $(n+1)$-cross-polytope, containing $K_{n+2} - P_2$, will appear as such skeleton; all of them are embeddable graphs of diameter two. For example, $K_7 - P_2$ appears as the skeleton of an n-manifold of type (ii), but only for $n = 4$.